Biol. Cybern. 57, 217–231 (1987)

Biological Cybernetics

A Model of the Motor Servo: Incorporating Nonlinear Spindle Receptor and Muscle Mechanical Properties

C. C. A. M. Gielen[1] and J. C. Houk[2]

[1] Department of Medical and Physiological Physics, Rijksuniversiteit Utrecht, Fysisch Laboratorium, Princetonplein 5, NL-3584 CC Utrecht, The Netherlands
[2] Department of Physiology, Northwestern University, Medical School, 303 East Chicago Avenue, Chicago, IL 60611, USA and Rehabilitation Institute of Chicago, 345 East Superior Street, Chicago, IL 60611, USA

Abstract. A model for the stretch reflex is proposed incorporating a nonlinear description of muscle receptor behavior, a delay in the reflex loop and a model of muscle mechanical properties. The model adequately describes the nonlinear response properties of EMG and force to constant ramps in loading and unloading direction. The EMG responses during the ramp and at ramp plateau could be simulated adequately for all ramp velocities except for high stretch velocities where EMG activity appeared in bursts, presumably due to spinal nonlinearities. Force responses during ramp stretches could be simulated except at ramp plateau, where the measured force response decayed slower than the simulated responses. The model also explained that EMG and force responses during ramp stretches after a displacement of about 1 cm could be approximately described by a product relationship between a position-related term and a low-fractional power of velocity. During unloading ramps the model did not predict a clear velocity dependence in agreement with the data.

1 Introduction

Stretch and unloading reflexes are mediated by a feedback system called the motor servo (cf. Houk 1979), consisting of a muscle, its stretch receptors and their reflex pathways back to the muscle. Our mechanistic understanding of these reflexes is based mainly on animal experiments where muscles, receptors and reflex pathways can be studied in functional isolation (Matthews 1972; Houk and Rymer 1981). Analogous reflexes in human subjects, elicited by loading and unloading joints, are thought to be mediated by composite motor servos consisting of synergistic groups of muscles and their interactive reflex pathways. Most research efforts so far have investigated the linear dynamic aspects of the motor servo and have shown that these aspects are accounted for by properties of receptors, reflex loops and muscles as revealed in reduced animal preparations (Stein 1974; Oguztoreli and Stein 1976; Bawa et al. 1976; Rack 1981). However, much less is known about the nonlinear dynamical properties of the motor servo.

Recent results indicate that the motor servo does in fact have prominent nonlinear dynamics, and these features may have substantial functional significance (Houk et al. 1981b; Aldridge and Stein 1982; Gielen and Houk 1984). Several of the unique properties of the motor servo, such as a dependence of EMG and force responses on a low fractional power of velocity (Gielen and Houk 1984), resemble nonlinear properties described for muscle spindle receptors (Houk et al. 1981a). Other features, such as the presence of a short-range region of high stiffness, may have a muscle mechanical origin as well (Joyce et al. 1969). In order to explore these possibilities, we have sought to develop a model of the motor servo that incorporates the major nonlinear and dynamical properties presented by muscles, muscle receptors and reflex pathways. We reasoned that this model, if it could be made sufficiently realistic, would serve several functions. First, it would provide a direct test as to whether known nonlinearities of muscle spindle receptors and of muscle contractile tissue are capable of explaining the major nonlinearities present in the overall properties of the motor servo. Second, it might provide a basis for calculating useful internal variables and parameters that are not accessible to direct measurement. Third, one might use the model to study potential mechanisms whereby descending motor command signals are converted into movements.

The responses of muscle spindle receptors were once thought to be represented by a superimposition of components proportional to muscle length, stretch velocity and acceleration. Later studies (Lennerstrand

1968; Lennerstrand and Thoden 1968) presented evidence against the idea of superimposition and suggested some kind of "dry friction" in the intrafusal muscle elements. This notion was supported by the observation (Cussons et al. 1977; Matthews and Stein 1969; Poppele and Bowman 1970; Hasan and Houk 1975b) that the sensitivity of muscle spindle primary endings is far greater for small than for large stretches. Subsequently, it was found that the responses of muscle spindles, both primary and secondary endings, bear a fractional power relationship to velocity and that velocity sensitivity is multiplicative with length sensitivity, rather than the two terms being additive (Houk et al. 1981a). These various data represent highly unique dynamical properties that are remarkably well captured by Hasan's (1983) nonlinear dynamical model of the muscle spindle. Hasan's model is the main ingredient of the representation proposed here for the reflex loop.

Various models of muscle have been proposed by different authors. Many of them incorporate well-known macroscopic nonlinearities, such as the force-velocity relationship (Hill 1938) and the length-tension relation. However, most models do not account for the actual forces that occur during lengthening contractions. The difficulty has been that of replicating the region of short-range stiffness and the abrupt reduction in stiffness that occurs after modest amplitudes of stretch (Joyce et al. 1969). Recently, a model that captures these phenomena has been proposed by Zahalak (1981), which basically is a modification of Huxley's two-state sliding filament model (Huxley 1957). Zahalak's model uses a distribution-moment approximation of crossbridge kinetics that is very economical to simulate, thus making it suitable for incorporating as a component in more global models of motor systems. This model, preceded by a first-order low-pass filter simulating the effect of diffusion of calcium ions on the activation of muscle, has been used in the present study. A preliminary communication of these results has been reported (Houk and Gielen 1986).

2 Methods

2.1 Experimental Procedures

The parameters of the model presented in this paper are fitted to EMG and force responses of the wrist musculature in human subjects. These stretch and unloading reflexes in response to ramp changes in wrist position were described in a previous paper (Gielen and Houk 1984), although some additional data were collected with the same apparatus for the purposes of the present report. A brief description of this apparatus is given here.

Subjects were seated in a chair with the lower arm in a horizontal position firmly held in a mold. The subject's relaxed hand was strapped to a handle. The distance from the point of fixation of the handle at the hand and the point of rotation in the wrist was about 8 cm. The handle was attached to a mechanical stimulus generator designed to control position. Force exerted by the wrist was measured with strain gauges located between the stimulus generator and the handle with a resolution better than 0.06 N. Position was measured by a linear potentiometer with a resolution better than 0.2 mm. Over the range studied (± 5 cm from the rest position), the forces and lengths of wrist flexor muscles are well approximated by proportional relationships with the measured force and position of the apparatus. The muscle fibers in the contractile part of m. flexor carpi radialis were assumed to be 10 cm long. The tendon was assumed to cross the wrist joint at a distance of 2 cm from the axis of rotation in the wrist. With these data, muscle force was transformed into force exerted by the hand at the handle. Moreover, these data were used to convert position and velocity at the handle to sarcomere length and sarcomere shortening or lengthening velocity, that were the inputs for the muscle mechanical model.

EMG signals were recorded with bipolar surface electrodes which were placed approximately above the endplate region of m. flexor carpi radialis and extensor carpi radialis (longus and brevis). After preamplification, signals were band-pass filtered (30 Hz–10 kHz), full wave rectified and low-pass filtered. Due to the presence of a preload in flexion, the extensor carpi radialis was silent or minimally active under the conditions of these experiments.

Stimuli were constant velocity lengthening or shortening ramps that stretched or unloaded the initially preloaded wrist flexor muscles. Before each trial the apparatus forced the wrist to a particular position. Force exerted by the wrist in that position was fed back to the subject by a cursor on an oscilloscope, and the subject's initial task was to hold the cursor in the window displayed on the oscilloscope screen. Then the force display on the oscilloscope disappeared and, after a variable time chosen in the range of 500–1000 ms, the lengthening or shortening ramp started. In order to minimize voluntary reaction components, the subject was instructed not to intervene voluntarily and nonintervention was monitored using the trial comparison method (Gielen et al. 1984).

2.2 Simulation of EMG Responses

The model used to simulate reflex-induced EMG activation of muscle consists of the three component processes outlined in Fig. 1A. Muscle length $x(t)$ is

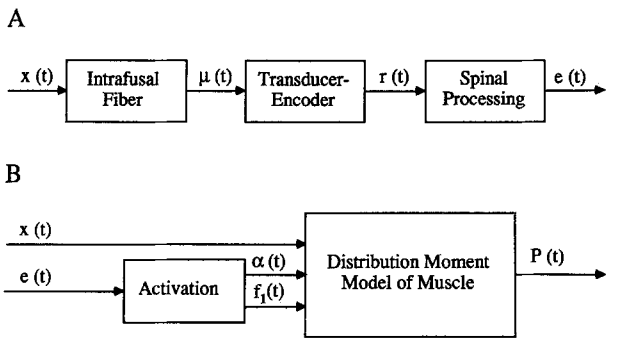

Fig. 1A and B. Block diagram of the model used to simulate reflex-induced EMG activation of muscle (**A**) and muscle mechanical responses (**B**). Muscle length $x(t)$ is mechanically filtered by intrafusal muscle fibers to produce a stretch of the sensory zone $\mu(t)$. Modification by a transducer-encoder process results in a discharge rate $r(t)$, which after spinal processing and a time delay of 0.03 s produces an EMG signal $e(t)$. Increases in $e(t)$ increase the fraction of motor units recruited $\alpha(t)$ and their firing rates $f_1(t)$. This activation together with muscle length changes $x(t)$ determines force output $P(t)$ of the distribution moment model of muscle

mechanically filtered by intrafusal muscle fibers in spindle receptors to produce a stretch of the sensory nerve ending $\mu(t)$. A transducer-encoder process converts nerve ending stretch into discharge rate $r(t)$ of the afferent nerve fiber. This afferent nerve signal is conducted to the spinal cord where it is processed and sent back to the muscle to produce an electromyographic signal $e(t)$ specifying the degree of muscle activation.

We adopted Hasan's (1983) model of the intrafusal fiber, since this model replicates the variety of nonlinear dynamical properties that have been described for primary and secondary endings in muscle spindles. According to this model, the length of the sensory zone μ as a function of muscle length x is given by the nonlinear differential equation:

$$\frac{d\mu(t)}{dt} + a\left(\frac{b\mu(t) - x(t) + c}{x(t) - \mu(t) - c}\right)^3 = \frac{dx(t)}{dt}, \quad (1)$$

where a and b are constants that affect the degree of nonlinearity in this differential equation and c is a reference length specifying the lower bound of the position range where the muscle spindle responds to stimuli.

We also adopted Hasan's formulation of the linear dynamics of the transducer-encoder process.

$$r(t) = H\left(\mu(t) + \tau\frac{d\mu(t)}{dt}\right), \quad (2)$$

where H represents the small-signal sensitivity of the receptors (plus additional constants described below) and $\tau = 0.1$ s is the time constant of encoder dynamics.

The reflex pathway through the spinal cord was simply modeled as a time delay of 0.03 s, based on the results of Gielen and Houk (1984).

$$e(t) = r(t - 0.03). \quad (3)$$

The parameters a and b depend on the type of ending and on the degree and type of fusimotor activity (Hasan 1983). These two parameters, together with the parameters H and c were adjusted to obtain the best least squares fit for the EMG responses to all ramp velocities in a given experiment. Since H is just a scaling factor, we included in its value the proportionality factor relating muscle length to wrist position and the gain of the reflex pathway, in addition to the sensitivity of the receptors. The value of H thus depends on wrist geometry, the amplification of EMG signals, position of electrodes, etc. and has no particular physiological relevance for this study.

The simulations were done on a PDP 11/40 and a HP 1000 computer. The average EMG activity in the period of one second preceding the ramp was used to estimate the baseline EMG on which the ramp response is superimposed. For the simulations of the EMG responses with the Hasan model, position $x(t)$ and velocity $dx(t)/dt$ of the wrist were used as the input. For position and velocity at a particular time, $d\mu(t)/dt$ was calculated with (1) using the present value of $\mu(t)$. With this value for $d\mu(t)/dt$, a new value for $\mu(t)$ was calculated using the relation $\mu(t) = d\mu(t)/dt^* \Delta t$ where Δt represents the time interval between successive computation steps. Then the EMG response was calculated using (2) and (3). The time increment Δt in the calculations was 0.1 ms.

Each simulation started with a particular value for the parameters H, a, b, and c. For this set of parameter values, the sum of the mean square error between the simulated and predicted responses for all ramp velocities was calculated. Then the parameter values were changed systematically until the least mean square error was obtained. The smallest increments and decrements for the parameters H, a, b, and c in this procedure were 0.01, 0.001 (cm/s), 1 and 0.1 cm, respectively.

2.3 *Simulation of Force Responses*

Figure 1B outlines the model used to simulate muscle force responses $P(t)$. One input to this model was $x(t)$, the time course of muscle length change, yielding the muscle mechanical response. The other input was $e(t)$, the simulated EMG response, yielding the neurally mediated component of the force response. The muscle mechanical response has both active and passive components. The passive elasticity was determined by experiments as 0.5 N/cm. The active component of

muscle mechanical behavior was simulated with a kinetic model of crossbridge mechanics.

Huxley's and other related kinetic theories on muscle contraction require the solution of the distribution function $n(y(t), t)$, which describes the fraction of actin-myosin bonds with length $y(t)$ at time t:

$$\left(\frac{\partial n}{\partial t}\right)_x - v(t)\left(\frac{\partial n}{\partial y}\right)_t = f(y) - [f(y)+g(y)]\, n(y,t), \tag{4}$$

where $f(y)$ and $g(y)$ are the rate parameters which give the probability of making ($f(y)$) or breaking ($g(y)$) of a bond with length $y(t)$ per unit of time. $v(t)$ represents the rate of change of sarcomere length y caused by the wrist velocity $\mathrm{d}x(t)/\mathrm{d}t$. The force of contraction $P(t)$ is then calculated from the first order moment of the distribution function

$$P(t) = \alpha C \int_{-\infty}^{\infty} y n(y,t)\, \mathrm{d}y, \tag{5}$$

where α is the degree of muscle activation and C is a constant that depends on parameters such as bond stiffness, sarcomere spacing, cross-sectional area (Zahalak 1981) and wrist geometry.

The solution of (4) requires large computational effort even for simulations of simple experiments. The model for muscle behavior presented by Zahalak (1981) is based on the assumption that only the distribution function and its first two moments are needed to describe macroscopic muscle behavior. This reduces the problem to solving a set of three first-order differential equations

$$\frac{\mathrm{d}M_0}{\mathrm{d}t} = b_0 - F_0(M_0, M_1, M_2), \tag{6}$$

$$\frac{\mathrm{d}M_1}{\mathrm{d}t} = b_1 - F_1(M_0, M_1, M_2) - \frac{\mathrm{d}y}{\mathrm{d}t} M_0, \tag{7}$$

$$\frac{\mathrm{d}M_2}{\mathrm{d}t} = b_2 - F_2(M_0, M_1, M_2) - 2\frac{\mathrm{d}y}{\mathrm{d}t} M_1, \tag{8}$$

where $M_i(t)$ is the i-th order moment of the distribution function $n(y,t)$ and b_i is the i-th order moment of the bond formation function.

The exact forms of the functions F_0, F_1, and F_2 depend on the rate functions $f(y)$, $g_1(y)$, $g_2(y)$, and $g_3(y)$ (for an exact formulation of these functions see Appendix in Zahalak 1981). The function $f(y)$ describes the probability to create a bond of length $y(t)$ per unit of time and is assumed to be directly proportional to the activation of muscle. The rate functions $g_1(y)$, $g_2(y)$, and $g_3(y)$ describe the probability per unit of time for breaking of a bond with length $y(t)$. The function $g_3(y)$ is not included in Huxley's original formulation; Zahalak (1981) introduced it to account for short-range stiffness and yielding. If h represents half the sarcomere length, these rate parameters are defined by

$$f(y) = \begin{cases} 0 & -\infty < y < 0 \\ f_1 y/h & 0 < y < h \\ 0 & h < y < \infty, \end{cases} \tag{9}$$

$$g(y) = \begin{cases} g_2 & -\infty < y < 0 \\ g_1 y/h & 0 < y < h \\ g_1 y/h + g_3(y/h - 1) & h < y < \infty. \end{cases} \tag{10}$$

The dynamics of the actin-myosin bonds were simulated with 20 μs time intervals for each next step in the simulation.

We let the EMG signal $e(t)$ act on the distribution-moment model of muscle through an activation process (Fig. 1B) consisting of a first-order low-pass filter with a time constant of 0.04 s to simulate the time constant for calcium release in muscle. The output of this process affected the muscle model in two ways, mimicking rate modulation of individual motor units and recruitment of additional motor units. Rate modulation was modeled by letting the parameter f_1 which gives the probability per unit of time to create an actin-myosin bond be proportional to the EMG activity. The bonding rate parameter f_1 in the Zahalak model was set at $15(\mathrm{s}^{-1})$ at ramp onset for ramp stretches starting from a relatively small preload (6 to 10 N). For unloading ramps starting from a higher preload (40–50 N), f_1 was set to 25 to $30\,(\mathrm{s}^{-1})$. The change in firing rate of motor units was simulated by changing this bonding rate parameter, f_1, as a function of EMG by the relationship

$$f_1(t) = 15 + \frac{[e(t) - e(o)]}{[e_{\max} - e(o)]}(35 - 15) \tag{11}$$

such that f_1 equals the maximal firing rate of motor units during maximal isometric voluntary contractions, which is about $35\,(\mathrm{s}^{-1})$ (DeLuca et al. 1982a, b). For all simulations, the rate parameters g_1, g_2, and g_3, which represent the unbonding rate parameters at different regions of sarcomere length, were set at 10, 210, and $100\,(\mathrm{s}^{-1})$, respectively, in agreement with the values used by Zahalak (1981).

The effect of recruitment of new motor units was simulated by letting α in (5) be a time function $\alpha(t)$ that increases proportionally with $e(t)$. The parameter C was then chosen such that the muscle model produced the measured initial force $P(0)$ in response to initial EMG $e(0)$ and the maximum isometric force [when $e(t) = e_{\max}$] measured during maximal voluntary contraction.

3 Results

Reflex responses of human subjects to ramp changes in wrist position show a nonlinear dependence on stretch velocity and a multiplicative relation between position and velocity sensitivity (Gielen and Houk 1984). EMG and force responses to stretch do not scale with stretch velocity, but instead increase as the 0.3 power of velocity for EMG and as the 0.17 power for force, and responses to release show almost no dependence on velocity. This characterization of velocity sensitivity multiplies with a linear position sensitivity component. A similar relationship is seen for soleus muscle reflexes in decerebrate cats (Houk 1981). Here we propose a model that characterizes these nonlinearities and other prominent features of the human wrist reflexes. Since muscle spindle receptors exhibit similar nonlinearities (Houk et al. 1981 b), we used Hasan's (1983) nonlinear dynamical model of the muscle spindle as a key component in our model of the reflex loop [Fig. 1 A and (1) and (2)].

3.1 *Characterization of the Reflex Loop*

The nonlinear differential equation characterizing mechanical filtering by intrafusal muscle fibers [Fig. 1 A and (1)] computes the hypothetical stretch of spindle nerve endings $\mu(t)$ that results from imposed changes in muscle length $x(t)$. [The actual input for the experimental responses to which the model was fitted was wrist position, which over the range studied is proportional to muscle length (Methods).] While no general solution of this equation for ramp responses has been found, analytic expressions for steady-state, initial and asymptotic responses have been derived (Hasan 1983), and their extension to the model of the entire reflex loop is presented here.

The steady-state response of (1) to a maintained muscle length $x(t)=x_{ss}$ is obtained by setting $d\mu(t)/dt = dx(t)/dt = 0$ in (1). This yields $\mu_{ss}=1/b^*(x_{ss}-c)$. The steady-state response of the remainder of the reflex model is simply the gain factor H, yielding the overall expression

$$e_{ss}=\frac{H}{b}(x_{ss}-c). \tag{12}$$

This relation is plotted as a static response component in Fig. 2 A (dot-dash line). Because of a relatively large value of b compared to the displacement $x(t)$ of the wrist, the static component is very small compared to the total response during ramp stretch.

The initial response at ramp onset has high sensitivity and follows linear dynamics. Assuming that a steady state was reached in the prestimulus interval, the nonlinear term in (1) is zero at ramp onset, and $d\mu/dt$ will equal the stretch velocity dx/dt. After the delay of 30 ms in the reflex loop, the model responds with a step-wise increase equal to $\tau H(dx/dt)$ (trace 1 in Fig. 2 A). The response continues as a linear increase with a slope determined by H. Thus H represents the small-signal position sensitivity of the loop corresponding to the linear, high-sensitivity region of spindle receptor responses (Matthews and Stein 1969; Poppele and Bowman 1970). This sensitivity is a factor b greater than the steady-state sensitivity given in (12).

After a certain amount of stretch, depending on the value of the parameters a and b, the changes in $\mu(t)$ and $x(t)$ will affect the nonlinear cubic term in (1). This term will grow in value until it is no longer small with respect to dx/dt. Then the $d\mu/dt$ term will decrease since the nonlinear term is always positive for ramp stretches. For large values of a and b the nonlinear term will become important at earlier phases during the ramp. For example, trace 4 in Fig. 2 A shows the result of a 2.7 fold increase in b; this change would also decrease the steady-state response which is not shown. Trace 2 in Fig. 2 A shows that a decrease in the value of a produces an extension of the small-signal region.

Changes in the values of a and b also affect the slope of the response later in the ramp (Fig. 2 A, traces 2 and 4). Inspection of (1) suggests that large values of a and b will give rise to a larger nonlinear term, which should result in smaller values of the slope of the response as soon as this term becomes important. Hasan (1983) has derived a relation which describes the asymptotic behavior of the spindle at constant stretch velocity. From this, the asymptotic response of the reflex loop can be written as

$$e(t)=\frac{H}{b}[1+m]\left[x(t-0.03)-c+\tau\frac{dx(t-0.03)}{dt}\right], \tag{13}$$

where m is a parameter that depends in a complex manner on velocity and the parameters a and b. However, for a range of low and moderate velocities, m is well approximated by the quantity $[(dx/dt)/a]^{1/3}$. Approximate asymptotic responses are plotted as dashed lines in Fig. 2 A. Increasing the value of the parameter a decreases the slope of the asymptotic response. Curve 2 in Fig. 2 A instead shows the effect of a 3 fold decrease in a. Changing the value of parameter c (Fig. 2 A, curve 3) gives rise to a horizontal shift of the line describing the asymptotic response.

The effect of parameter H is just a scaling of the simulated EMG response, and its effect on the responses of the model is not shown in Fig. 2 A.

At ramp plateau, when the velocity dx/dt becomes zero, the rate of change of $\mu(t)$ in (1) will become negative to balance the current value of the nonlinear

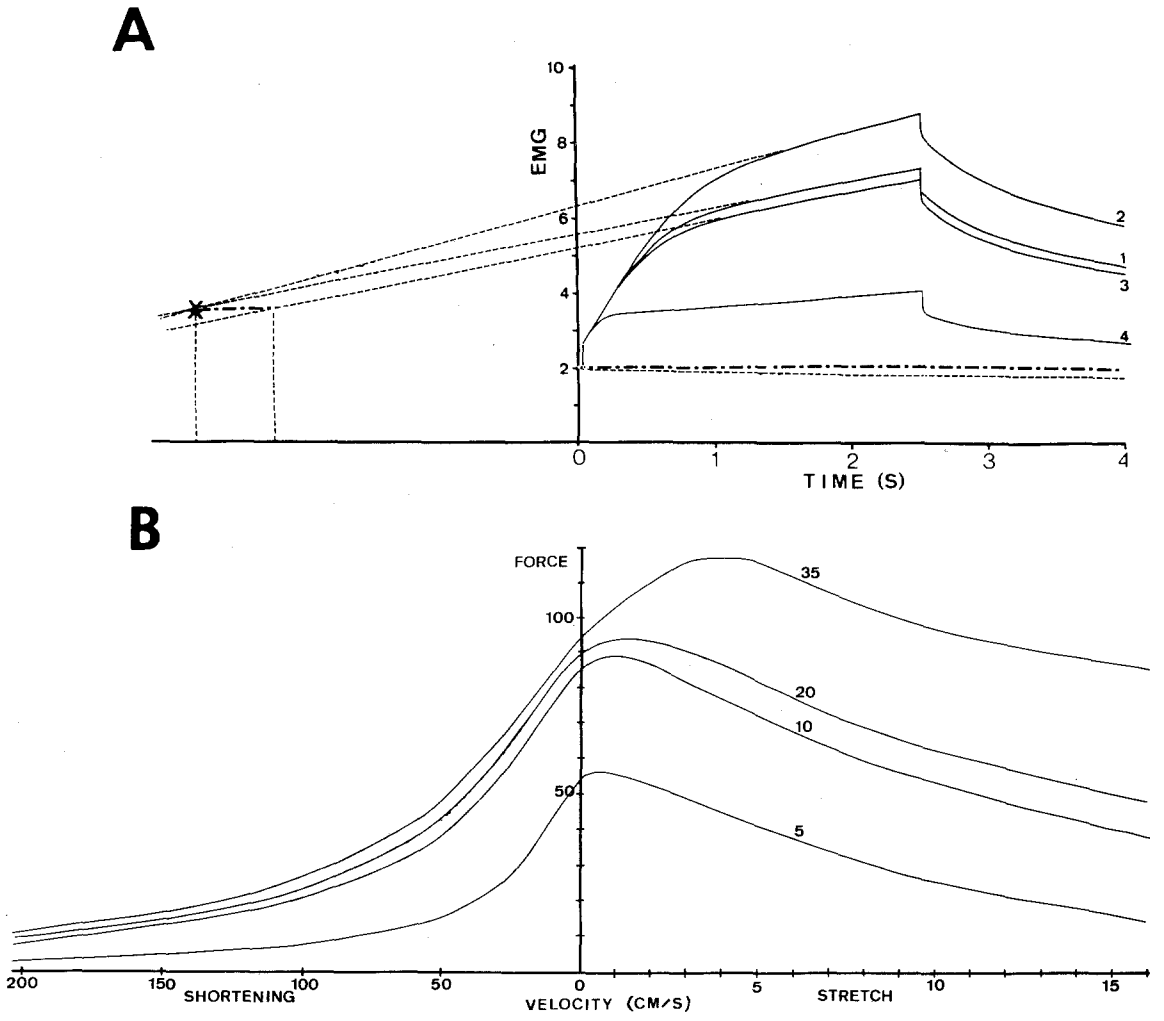

Fig. 2A and B. Properties of the model. **A** Simulated EMG responses to ramp stretches of 2 cm/s for different parameter values of *a*, *b*, and *c*. Trace 1 shows the response for values for *H*, *a*, *b*, and *c* of 3, 0.003 (cm/s), 75 and −1.5 (cm). After a small delay of 30 ms, the response increases abruptly due to the step-like increment of stretch velocity. Then the response increases with a slope which after about 0.5 s (corresponding to 1 cm of stretch) decreases gradually until it becomes constant and approaches the asymptotic response (broken line) given by (13). Decreasing the value of a to 0.001 (cm/s) (trace 2) does not affect the initial part of the response, but gives rise to a more gradual decay of slope and a steeper slope of the asymptotic response. Larger values for *c* ($c = -0.5$ cm; trace 3) lead to an earlier decay of the slope and to smaller response values corresponding with a shift of the asymptotic response. Increasing the value for *b* to 200 (trace 4) leads to an earlier departure of the initially steep slope and to a smaller slope of the asymptotic response. The steady state response given by (12) is shown by the thick dot-dash line. It increases linearly from the baseline EMG (thin broken line) until the end of the ramp and remains constant after that. **B** Force-velocity relationship for shortening and lengthening velocities as predicted by the Zahalak model for four values of muscle activation. Model parameters: $f_1 = 5, 10, 20$, and 35 (s^{-1}); $g_1 = 10$ (s^{-1}), $g_2 = 210$ (s^{-1}), and $g_3 = 100$ (s^{-1}). Note the different velocity scale for lengthening and shortening velocities (see text for explanation)

term, the latter functioning as a storage element that must be dissipated over time. As a consequence of the cubic relationship, $\mu(t)$ will decay very slowly toward the steady state value given by (12). The decay becomes faster for larger values of *a* and *b*. In addition to this slow decay, the reflex loop responses (Fig. 2A) exhibit an initial rapid drop due to linear dynamics equal to the term $\tau H(dx/dt)$ in (2).

Figure 3A–D shows a typical result of fitting model parameters to EMG ramp-lengthing data. Before the ramp started, the wrist opposed an initial preload of 6 N in the extension direction loading the wrist flexor muscles. The measured EMG traces show the previously described velocity dependence, namely that EMG increases with ramp velocity but less than proportionally. The parameters *a*, *b*, *c*, and *H* were adjusted (Methods) to obtain a good fit to the stretch phase of the response for all velocities, and the result is shown by the agreement between experimental and simulated responses superimposed in Fig. 3A–C. The

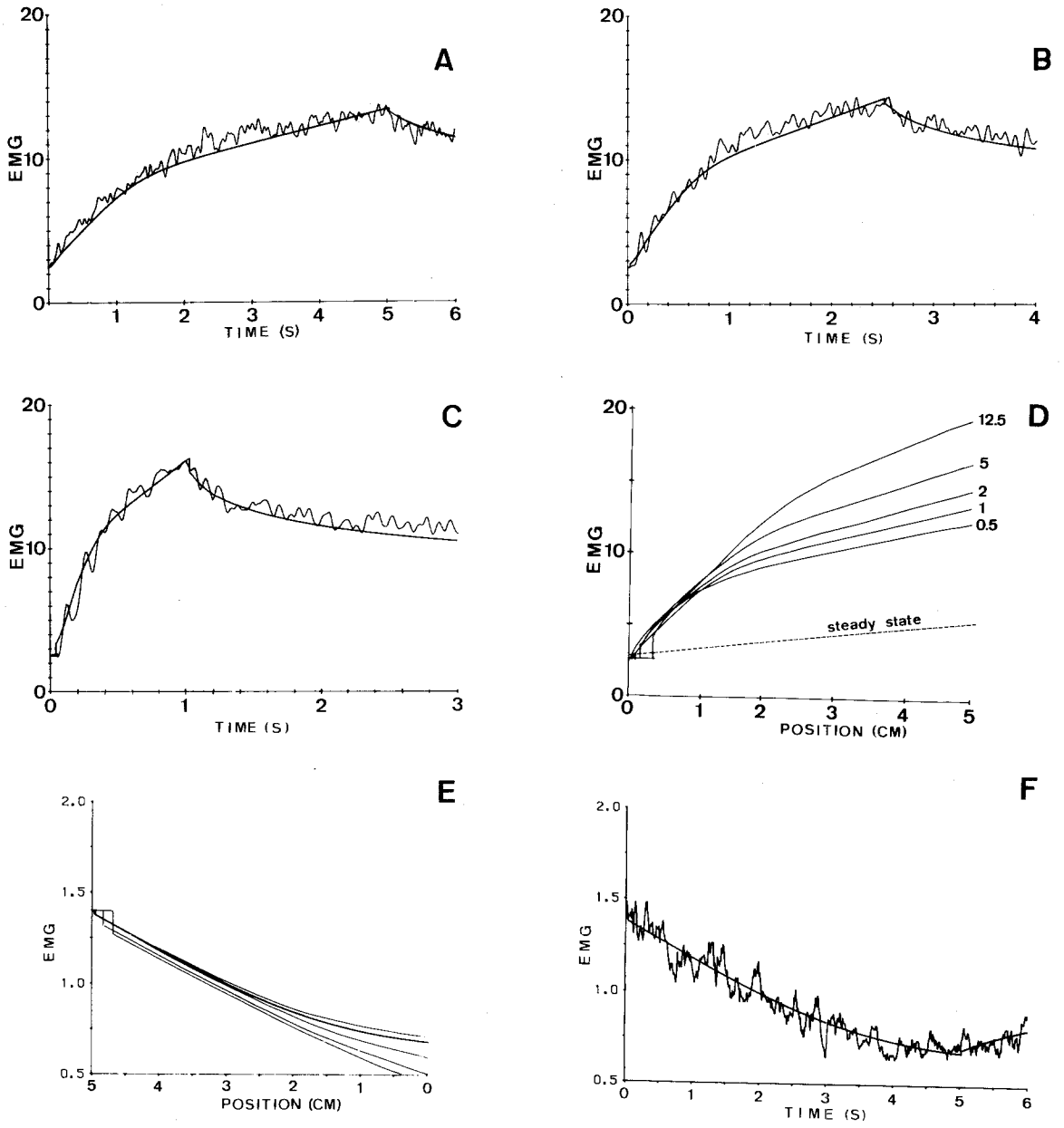

Fig. 3A–F. Comparisons of model with EMG data. **A–C** shows measured and simulated EMG responses to ramp stretches pf 1, 2, and 5 cm/s. Each experimental trace is the average of 15 responses. **D** shows a set of simulated EMG responses for different stretch velocities (0.5, 1, 2, 5, and 12.5 cm/s) as a function of position. Broken line indicates the steady state response given by (12). Due to the delay of 30 ms in the reflex loop the position of response onset increases with ramp velocity. Parameter values used for all simulations: $a=0.004$ (cm/s), $b=75$, and $c=-2.5$ (cm). **E** Simulated EMG responses to unloading ramps at velocities 0.5, 1, 2, 5, and 10 cm/s. **F** Comparison of measured and simulated EMG response for an unloading velocity of 1 cm/s. Parameter values used in all simulations: $a=0.003$ (cm/s), $b=75$, and $c=-3$ (cm)

excellent fit to the slow adaptation at ramp plateau results from the predictive power of the model, since this phase of response was not used in the parameter estimation procedure.

Figure 3D compares simulated responses at different stretch velocities, using plots of EMG response versus position. The weak velocity dependence of the asymptotic phase of response is evident for stretch amplitudes in the 2–5 cm range. The initial response phase (up to 1 cm) shows minimal dependence on velocity for two reasons. The first is that neither the velocity dependence resulting from linear dynamics (2) not that resulting from nonlinear features is very prominent in this velocity range. The second is that this small velocity dependence is counteracted by the 30 ms delay in the reflex loop.

EMG ramp-shortening data show two prominent differences from ramp-lengthening data. First there is little velocity dependence other than that accounted for by delay in the reflex loop (Fig. 6 of Gielen and Houk 1984). This feature is also present in the model as shown in Fig. 3E. As with ramp lengthening, the nonlinear term in (1) is initially zero, but in this case it grows (here becoming negative) about 3 times more gradually (for the values of a, b, and c used to fit corresponding ramp-lengthening data) than it does with ramp lengthening. Therefore, the responses for ramp shortening do not have a clear change of slope until toward the end of the response (Fig. 3E). Figure 3F shows a comparison between measured and predicted response at a stretch velocity of 1 cm/s. Though not fully shown, the EMG response at ramp plateau is also adequately explained by the model. The adaptation phase is slow both for the model and the experiment.

The other prominent difference in the shortening versus lengthening data is the existence of about a twofold reduction in sensitivity. The model as it stands does not explain this difference, though we are able to account for it by reducing the gain factor H to a value less than that used to fit ramp-lengthening responses. Possible justifications for changing this parameter during shortening are outlined in the Discussion.

Results similar to those shown in Fig. 3 have been obtained for five subjects. The parameter values for a, b, and c which gave the best fit for the EMG responses were very similar for all subjects. These values were in the range from 0.001–0.005 cm/s for parameter a, 70–90 for parameter b and -4 to -1 cm for parameter c.

3.2 *Characterization of Muscle Mechanics*

Our approach to the characterization of force responses has been to use the simulated EMG responses described in the previous section as inputs to a representation of muscle that is based on Zahalak's (1981) moment-distribution model of crossbridge kinetics (Methods, Fig. 1B). Some modifications of the Zahalak model were necessary to account for the human reflex data. Assumptions regarding the activation process and the respective contributions of motor unit recruitment and rate modulation are detailed in Methods. We also found it necessary to scale lengthening and shortening velocities differently, as described below.

Figure 2B shows the force-velocity relationship predicted by the moment-distribution model. For shortening velocities, shown unconventionally to the left to facilitate later comparisons, the relationship shows the familiar decay of force with shortening velocity. For lengthening velocities, force initially increases and then starts to decrease for larger stretch velocities. Force-velocity data for the wrist flexor muscles show that force drops to 50% of the isometric value at shortening velocities of about 40 cm/s. If the Zahalak model fits this force-velocity relationship for muscle shortening, the model then predicts a peak in the force-velocity relationship for muscle lengthening near stretch velocities of about 10 cm/s. However, in order to fit our previous and present data, the peak in the force-velocity relationship for lengthening must occur at or below stretch velocities of 0.5 cm/s, as will be explained later. Thus, we have scaled the velocity sensitivity of the model for lengthening velocities by the factor 1/10, such that the peak in the force-velocity relationship for lengthening velocities occurs at 0.5 cm/s instead of at 10 cm/s. This modification is probably not in disagreement with other experimental data (Discussion).

Responses to ramp stretch of the complete model including muscle mechanical properties are shown superimposed on experimental responses in Fig. 4A. For both simulated and experimental traces, the initial slope of force increase is steep. This is due in part to the effect of short range stiffness of muscle and in part to the initially steep increase of the EMG response that was illustrated in Fig. 3A–D. After about 1 cm of stretch, the slope of the force response decreases to a lower value and remains approximately constant during the remainder of the ramp stretch. This change in slope is less prominent at higher velocities in both simulated and experimental traces.

While the stretch phase of the response is well explained by the model, a discrepancy between the measured force response and the simulated response occurs at ramp plateau. The force response in the model adapts faster than the measured response. Since the EMG response at ramp plateau is well explained by the model, this discrepancy for force is probably due to muscle mechanical properties which are not accounted for by the moment-distribution model of muscle (cf. Discussion).

A possible explanation for the slow decay of force was investigated by incorporating a tendon series elastic element into the model. After ramp offset the velocity of contractile element lengthening does not go immediately to zero, but instead decays toward zero while tendon elasticity undergoes stress relaxation. If the lengthening velocity in this phase drops to a value near the peak in the lengthening force-velocity relationship, muscle force will assume a value above isometric and decay slowly toward the latter. The result of this interaction between muscle and tendon elasticity is a longer time constant for decay of force similar to that observed by Joyce and Rack (1969)

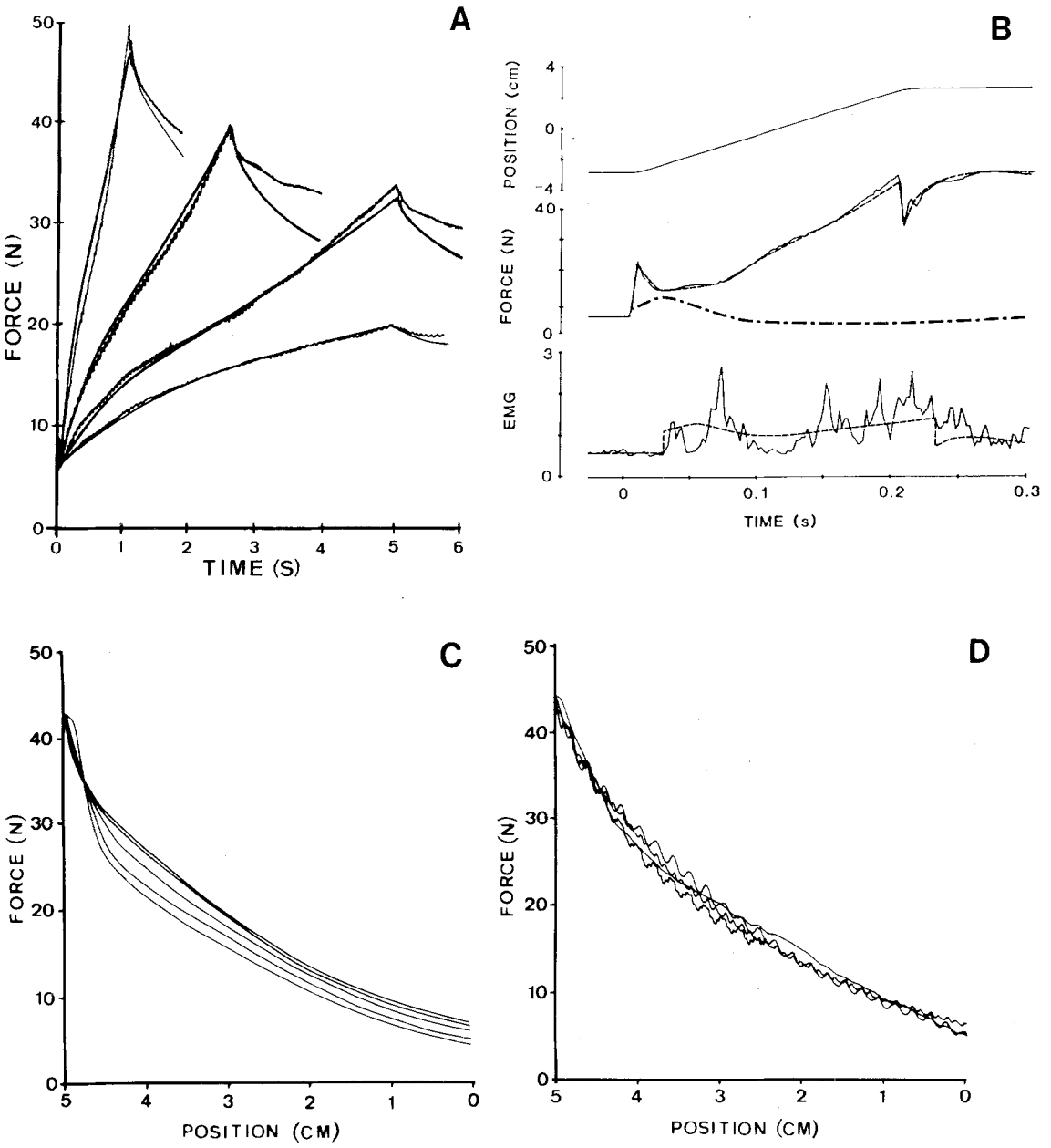

Fig. 4A–D. Comparisons of model with force data. **A** Measured and simulated force responses to ramp stretches at different velocities (1, 2, 5, and 12.5 cm/s). The parameters used to simulate the EMG activity were $a=0.005$ (cm/s), $b=70$, and $c=-1.2$ (cm). The parameters for the Zahalak model were $f_1=15\,(s^{-1})$, $g_1=10\,(s^{-1})$, $g_2=210\,(s^{-1})$, and $g_3=100\,(s^{-1})$. **B** Measured (full line) and simulated (broken line) responses of force and EMG to a high velocity (25 cm/s) ramp stretch. The thick dot-dash line in the force section shows the simulated muscle mechanical response at constant activation after subtraction of inertial forces at ramp onset and offset. Simulation parameters for EMG were $H=0.5$, $a=0.002$ (cm/s), $b=-75$, and $c=-2$ (cm). **C** and **D** show force responses to unloading ramps at velocities 0.5, 1, 2, 5, and 12.5 cm/s. **C** Simulated responses. **D** Measured responses. Parameter values for EMG were $a=0.003$ (cm/s), $b=75$, and $c=-4$ (cm)

during isotonic lengthening and shortening movements of cat soleus muscle. However, simulation studies showed that even though the decay became slower as the spring constant of the series elasticity decreased, the experimental trace could not be simulated, not even if the value of the spring constant was a hundred times below that estimated for tendons (Rack and Ross 1984).

The effect of reflex activity on the responses at high stretch velocities is shown in Fig. 4B. The peak in the measured force trace at ramp onset and the dip at ramp offset are due to inertial force components, related to

the sudden acceleration and deceleration of the wrist. If inertial force components are neglected, force at constant activation initially increases (dash-dot curve in Fig. 4B), due to the short-range stiffness of muscle. After about 30 ms, muscle mechanical force peaks (yielding phase) and starts to decrease toward a level less than the preload value, as predicted by the force-velocity relationship shown in Fig. 2B. With reflex activity intact, force does not show the decrease in force, but rather increases slightly after 30 ms. This time corresponds with the arrival of the reflex activity in EMG which apparently compensates for muscle yielding. A larger force increase follows the second burst of EMG activity.

Figure 4B shows that the model accounts for the force responses adequately. However, for EMG some differences between measured and predicted responses do exist. The most prominent difference is the absence of periods of decreased activity after the peaks in EMG activity. This has been observed previously (Aldridge and Stein 1982) and has been ascribed to spinal nonlinearities that synchronize motor neuron discharge. Our results indicate that this synchronization of motor discharge has very little effect on force development. Correspondingly, we have not included these spinal nonlinearities in our model.

The force responses to shortening ramps are shown in Fig. 4C and D. All ramp releases started at a relatively high preload of 43 N in extension direction loading the wrist flexor muscles in order to avoid a contribution from the extensor muscles. Initially there is a steep decrease in force both in the simulated and measured responses. This rapid fall in force is probably due to the short-range stiffness of muscle and to series elasticity. In agreement with the observations in Gielen and Houk (1984) all force responses superimpose if plotted as a function of position. A similar behavior is obtained for the simulated responses. Since the effect of the force-velocity relationship of muscle becomes prominent only at relatively high shortening velocities, its effect on muscle force is very small for the velocities used here. However, there is a significant decrease of force for higher shortening velocities, which is for the larger part related to the small decrease of EMG responses for higher shortening velocities (see Fig. 3E and F). Summarizing, the most prominent effect of muscle on force responses to shortening ramps is the effect of short-range stiffness, which causes the initially steep decrease of force.

3.3 Fractional Power Dependence on Velocity

The asymptotic dependencies of EMG and force on velocity were compared for simulated and experimental responses. To reduce the effect of noise and variability in EMG, values were averaged over the range where wrist position increases from 2 to 3 cm of stretch, and all data points were corrected for the delay of 0.03 s in the reflex loop using the procedure described earlier (Gielen and Houk 1984). In agreement with our previous results (Gielen and Houk 1984), most of the points lay along a straight line on log-log plots, indicating a fractional power relationship to velocity. The exceptions were at the highest ramp velocities, where both the measured and simulated points deviated from a straight-line fit. This is explained by the fact that the power relationship to velocity is only an approximation to the actual asymptotic response of the model given by (13), which is valid for low velocities only. For higher velocities the predicted asymptotic response deviated from strict fractional power resulting in smaller responses. Another explanation is that for the highest ramp velocities used here, the response has not yet approximated the asymptotic response close enough and, therefore, does not quite fit to a power relationship.

The slopes of the stright-line fits were 0.24 and 0.17 for the EMG and force data, respectively, which is well in the range as reported earlier by Gielen and Houk (1984). These results suggest that the quantitative differences between the exponents of force and EMG relations might be explained by muscle mechanical properties.

The force-velocity plots in Fig. 5A and B were computed from the model in order to analyze the relative contributions of neural and mechanical mechanisms to the velocity sensitivity of the motor servo as a whole. Part A shows the entire ± 20 cm/s range explored in this study while part B shows an expanded view of the ± 2 cm/s range. The linear coordinates used here emphasize the nonlinearity of purely mechanical properties of MUSCLE and of reflexly induced changes in muscle activation (EMG), showing how these combine to yield the novel velocity dependence of total FORCE responses.

To facilitate comparison with force measures, the EMG graphs are scaled to reflect the force which would be produced if the muscle were isometric. The stretch velocity range illustrates the saturating nature of the approximate dependence on $v^{1/3}$, and the shortening range shows the near absence of velocity dependence under these conditions. The lower MUSCLE graph, in each part of the figure, illustrates how force would depend on velocity if there were no reflexly induced change in EMG. Throughout most of the range of lengthening, MUSCLE mechanical force is predicted to decrease with stretch velocity.

The FORCE graphs incorporate both neural and mechanical components. For the shortening range, reflex force closely parallels the MUSCLE component, because the neural component has very little velocity

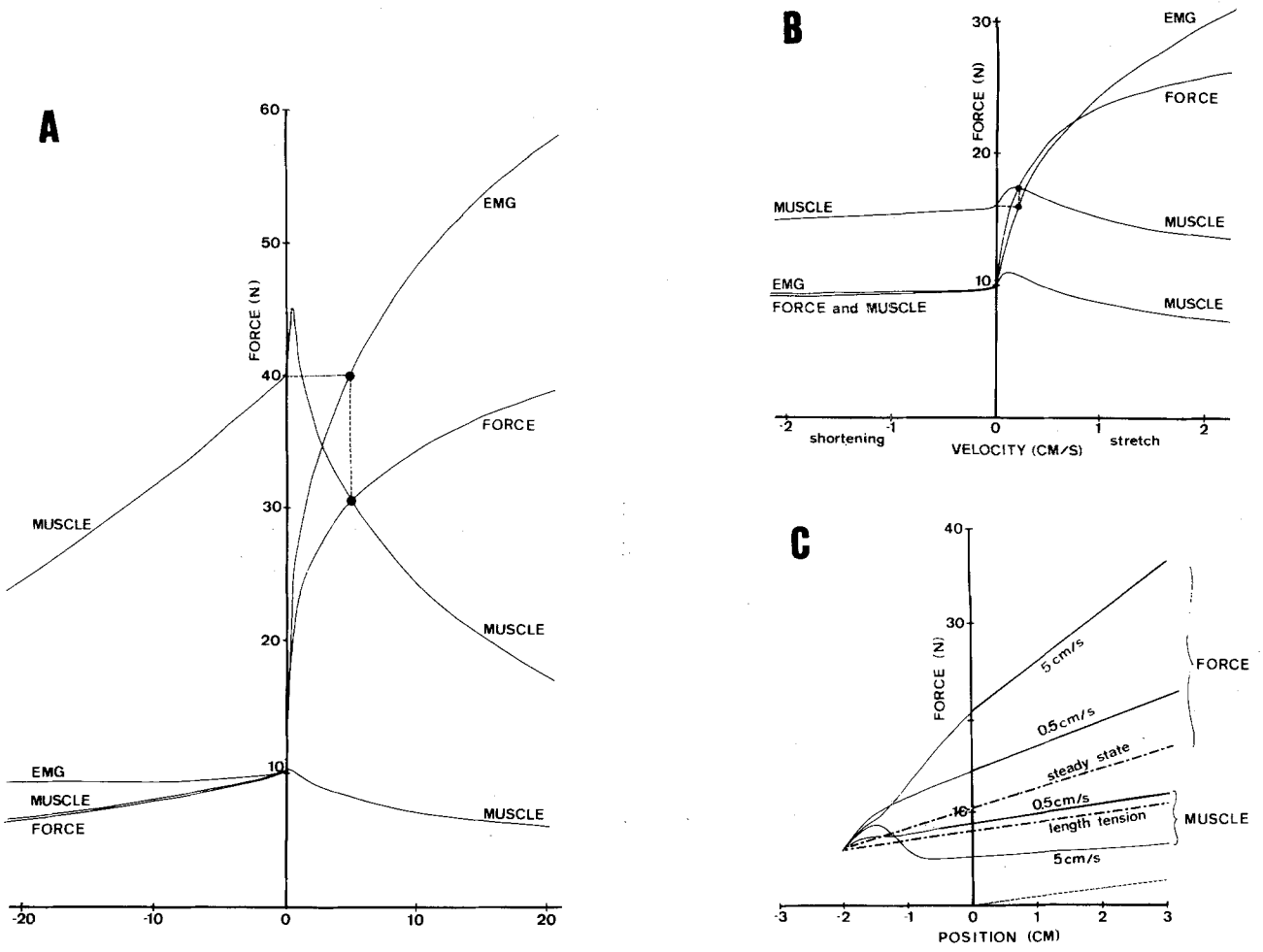

Fig. 5A–C. Force, velocity, position relationships of the model. Simulated force and EMG responses are shown for a large (**A**) and small (**B**) range of ramp velocities in shortening and lengthening direction. All values correspond to a single mid-position of the wrist. The curve labeled "EMG" is calibrated in equivalent isometric force units. Curves labeled "MUSCLE" indicate force at constant activation and represent pure muscle mechanical properties. The curve labeled "FORCE" represents total force including the neural component and muscle mechanical properties. Due to muscle force values exceeding isometric force at small stretch velocities, total force values exceed EMG expectations at stretch velocities below about 1 cm/s. For higher stretch velocities, reflex muscle yielding results in a force that is smaller than EMG expectations. For shortening velocities EMG activity does not depend on ramp velocity. Due to the force-velocity relation of muscle, the corresponding reflex force decreases with shortening velocity. **C** Force versus position plots of model responses at stretch velocities of 0.5 and 5 cm/s. Broken line starting from the central rest position indicates the passive length-tension relation for the relaxed wrist. Purely mechanical properties are shown by the responses labeled "MUSCLE" (constant EMG). For ramp velocities of 0.5 and 5 cm/s muscle force initially increases due to the short-range stiffness of muscle. After about 1 cm of stretch, muscle force remains higher than length-tension force for 0.5 cm/s and lower for 5 cm/s of stretch due to the force-velocity relation. With reflex activity, force increases considerably during stretch (responses labeled "FORCE"). Due to the delay in the reflex loop, force at the 5 cm/s stretch velocity is initially smaller than for the 0.5 cm/s stretch velocity. However, because of the higher EMG activity at larger stretch velocities, force at 5 cm/s exceeds force at 0.5 cm/s stretch after about 1 cm stretch

dependence. However, for the lengthening range, both neural and mechanical components are appreciably expressed. The graphical analysis shown in Fig. 5B illustrates how muscle mechanical effects slightly enhance the neurally mediated force component at low stretch velocities. The upper MUSCLE graph was computed under the assumption of an activation level equal to the value of EMG at 0.2 cm/s, and the vertical line segment at this velocity shows a small additive mechanical contribution to force. The graphical analysis in Fig. 5A instead illustrates how muscle mechanical effects appreciably decrement the neurally mediated force at higher stretch velocities. Here the upper MUSCLE graph was computed under the assumption of an activation level equal to the value of EMG at 5 cm/s, and the vertical line segment shows an

appreciable reduction in force due to muscle mechanics. The net result over the whole velocity range is a FORCE graph that depends approximately on $v^{0.17}$.

3.4 Product Relationship Between Position and Velocity

Figures 3A–D and 4A illustrate that the slopes of the asymptotic responses of both EMG and force responses increase modestly with stretch velocity. Similar findings have been reported for cat spindle receptor responses, and there it was clearly demonstrated that this augmentation in slope cannot be explained by a slow transient property (Houk et al. 1981a). Instead, it was concluded that a product relationship exists between position and velocity sensitivities. Evidence for a product relation was also found in our previous study of wrist reflexes in human subjects (Fig. 2 in Gielen and Houk 1984), and it is also a feature of the present model. The force-position plots in Fig. 5C were computed from the model in order to analyze the relative contributions of neural and mechanical mechanisms to this product relationship.

Figure 5C compares, for two velocities, the total FORCE responses with the purely mechanical responses of MUSCLE that would result if there were no reflexive increase in activation. The difference between the two sets of graphs is due to the neural component, which is appreciable at both stretch velocities. The dashed line estimates the passive elastic component that contributes to each of the other graphs. The length-tension curve applies to the level of activation present prior to the initiation of the lengthening ramp.

At the higher velocity, short-range stiffness of muscle is predicted to dominate the initial 0.5 cm of the FORCE response, whereas the delayed neural component arrives in a timely manner to mask yielding, similar to what has been observed in the decerebrate cat (Houk et al. 1981b). After yielding, the MUSCLE mechanical component falls below its isometric level whereupon it develops a weak position dependence. It is clear that the position dependence of the total FORCE response in the asymptotic phase is dominated by the neural component.

At the lower stretch velocity, the delay in reflex action is negligible. Short-range stiffness plays a lesser role, and the subsequent mechanical response has a small slope that parallels the muscle length-tension curve. The total FORCE of the reflex response shows a smooth transition from a high-stiffness region onto its asymptotic trajectory which is dominated by the neural component. In summary, the only part of the overall response that is accounted for by muscle mechanical forces is the initial portion, and then only at high velocities. Most response features are dominated by the neural component.

4 Discussion

The aim of this study was to investigate whether the nonlinear viscoelastic properties of the wrist motor servo could be explained quantitatively based on the physiologically known mechanisms that are involved in the reflex pathways. It was assumed that only properties of muscle and of relatively pure stretch reflexes were studied by instructing subjects not to intervene voluntarily to the imposed wrist displacements and by using the trial-comparison method described previously (Gielen et al. 1984). The trial-comparison method performs a pair-wise comparison between responses and selects a cluster with responses that deviate less than 5% from each other. The idea is that responses which contain unintended reactions of subjects are eliminated from further analysis, and that the remaining set of responses reflects muscle mechanical properties and pure reflex activity. This assumption is corroborated by experiments on decerebrate cats (Houk 1981) which have shown results similar to those obtained in this study. In the decerebrate cat both EMG and force responses, after the initial transient, can be described by a product relationship between position and a fractional power of velocity.

4.1 Simulation Results of EMG Responses

The model that was used to simulate EMG responses was based on a model originally proposed to describe the response properties of muscle spindle afferents. Contributions of other receptors, such as Golgi tendon organs, were not included in the model. The rationale for not including Golgi tendon organs was the small gain or absence of force feedback in the stretch reflex (Houk et al. 1970; Jack and Roberts 1978; Rymer and Hasan 1980). For other receptors the contribution to the stretch reflex is known to be small or nonexistent, or is unknown. Our simulation results show that muscle spindle activity may be sufficient to explain EMG and force responses to loading and unloading ramps.

The values for the parameters which were found to describe the EMG responses in this study were different from those proposed by Hasan (1983) to describe the behavior of cat soleus muscle spindles. One possible explanation may be a difference in species. However, another plausible explanation may be that the measured EMG response reflects the summed activity of all muscle spindles each with a different set of parameter values. In that case EMG has to be described by some combination of the parameter values of different muscle spindles, rather than by the parameter values of one single muscle spindle. Whether or not this is a satisfactory explanation

depends on the distribution of parameter values for muscle spindle afferents.

Initially all muscle spindle afferents demonstrate a steep increase in response at ramp onset. The slope of this part of the response is determined by the small-signal sensitivity of the muscle spindle afferent. Any combination of muscle spindle afferent responses will give a similar linearly increasing response.

The range of the high sensitivity region depends on the parameter values of a and b. For large values of a and b this region is small before the slope of the response decreases to a lower, approximately constant value (Fig. 2A). For small values of a and b, the high sensitivity region is larger and the slope decreases very gradually to a lower value. For the combined response, the amplitude of the high sensitivity region is determined by the muscle spindles with the largest values of a and b, and the region where the slope of the response decreases to a lower value is determined by the muscle spindles with the lower values for a and b.

If the parameter values for a and b for muscle spindle afferents show a rather homogeneous distribution, the combined response will demonstrate a gradual decrease of the slope of the response. If, however, this distribution would have been bimodal, the combined response would not show a gradual, but rather a fluctuating change of slope. Therefore, our observations suggest that muscle spindles do not form discrete populations, but rather show a continuous distribution of response properties, which is in agreement with previous observations (Wei et al. 1986). After a certain amount of stretch, the response asymptotes toward a straight-line relation when plotted as a function of position. Any combination of muscle spindle responses then will result in a straight-line relation for the combined response, which is in agreement with our results.

Although the model that was used to describe the EMG responses was based on the muscle spindle model proposed by Hasan (1983), this should not be understood to suggest that spinal mechanisms do not play an important role. Some clear differences between muscle spindle responses and EMG responses are present. For stretch velocities above 12.5 cm/s, the first part of the EMG response consisted of a sequence of bursts (see Gielen and Houk 1984). These bursting modulations could not be simulated by the model (Fig. 4B) and have been ascribed previously to spinal mechanisms, such a synchronisation of motoneuronal excitability cycles (Aldridge and Stein 1982). Moreover, it is well-known that muscle spindles demonstrate a high sensitivity for small stretch resulting in a pronounced burst of activity at ramp onset (Lennerstrand and Thoden 1968; Brown et al. 1969; Houk et al. 1973; Hasan and Houk 1975a). This burst in muscle spindle responses is present at relatively small stretch velocities, but was absent in the EMG responses at the corresponding stretch velocities.

Another difference between muscle spindle responses and the EMG responses described in this study concerns the fact that firing rate of muscle spindles drops to zero if unloading velocity is more than about $0.2\,l_0$/s (Prochazka 1981) or even $0.01\,l_0$/s (Crowe and Matthews 1964) depending on fusimotor activity, where l_0 refers to the rest length of the muscle. A similar behavior is not observed in the EMG responses (see Gielen and Houk 1984). EMG responses decrease approximately linearly with ramp position with only a slight velocity sensitivity.

Since the I_a-afferents in particular demonstrate an absence of response during muscle shortening, the position-related decrease of EMG activity during muscle shortening may suggest a more important role for secondary endings. The responses to stretch also better mimic the responses of secondary than of primary endings, since the dynamic index of EMG and force is relatively small compared to that observed for primary endings. This agrees with Matthews (1969), who found evidence that secondary endings contribute importantly to the stretch reflex in decerebrate cats.

As reported in the Results section, the parameter H in (2), which represents the gain of the reflex-induced EMG activity, is about twice as small for shortening velocities as it is for lengthening velocities. This difference seems to be significant, and a smaller response gain for shortening ramps has also been reported recently for EMG and I_a responses in cat (Carp et al. 1986). The latter results suggest that the difference in gain for lengthening and shortening responses is caused by nonlinearities in the I_a muscle spindle. Another argument, which adds to the lower response gain for EMG responses is that I_a afferents demonstrate an absence of activity during shortening, such that EMG during shortening may reflect activity from type II afferents only, in contrast to lengthening ramps where both types of receptors contribute to the response. Since type I_a and type II afferents are supposed to have different parameter values for a, b, and c, the fact that the parameter values for a, b, and c are the same for lengthening and shortening argues against an exclusive contribution of type II afferents during shortening.

4.2 Simulation Results of Force Responses

The model that was used to simulate muscle mechanical properties (Zahalak 1981) was able to explain most of the quantitative differences between responses of EMG and force. However, the muscle mechanical model cannot explain all features of the differences between EMG and force. First there is the observation

that the muscle mechanical model predicts the peak in the force-velocity relationship for muscle lengthening at too high a velocity. Data obtained for the human wrist during muscle shortening (S.L. Lehman and J.C. Houk, unpublished observation) demonstrate that force drops to 50% of the isometric value at a shortening velocity of about 40 cm/s. This value is in agreement with observations for muscle shortening in arm flexor muscles (e.g. Jørgensen 1976) if a correction is made for anatomical differences between wrist and arm muscles. Then, the model predicts the peak of the force-velocity relationship for lengthening at about 10 cm/s. However, the model cannot be fit to our data throughout the full range of stretch velocity unless the peak in the force-velocity relationship for muscle lengthening occurs at or below the velocity of 0.5 cm/s. If our data are converted to the muscle geometry for calf muscles, they are in agreement with the data of Bigland and Lippold (1954). These observations forced us to use a different velocity scaling in the moment-distribution model to mimic the experimental data on the force-velocity relationship for shortening and lengthening. Probably, more experimental data are necessary to resolve this issue, especially since most data on the force-velocity relationship for lengthening are obtained from muscles during high-frequency tetanic stimulation only.

Another imperfection of the model concerns the observation that the measured force responses at ramp plateau do not decay as fast as the simulated force response, even though the measured and simulated EMG responses fit nicely. This failure may be related to a not yet understood phenomenon of muscle behavior: the "permanent" tension which is found to be higher following an active stretch than it is during a fixed-end tetanus, even though the final end-to-end fiber length is the same (Abbott and Aubert 1952; Edman et al. 1976; Julian and Morgan 1979). This difference in force, which suggests some "memory" for the past behavior of crossbridges, is known to remain for a relatively long time, at least for several seconds, which is in agreement with our findings. Although suggestions have been made to explain this observation, more experiments are necessary to understand this muscle nonlinearity.

Despite these imperfections, the results show that the present model can give a quantitative explanation for the highly nonlinear response characteristics of the motor servo for both ramp stretches and releases as reported earlier (Gielen and Houk 1984). Most noteworthy is the ability of the model to account for the low fractional power dependence on velocity, the smaller velocity exponent of force as contrasted with EMG data, and the product relationship between position and velocity. These nonlinear features are not explained by previous models (see Introduction). In particular our results lead to the deduction that the product relationship between position and a fractional power of velocity is driven by the neural component of the reflex. The mechanical component serves mainly to provide an initial resistance to high velocities of length change and to reduce the exponent of velocity dependence from 0.3 power originating in spindle receptors to the 0.17 power present in overall motor servo properties.

4.3 Functional Implications of Nonlinear Viscosity

Several mechanisms have been proposed to give the stretch reflex properties such that the motor servo acts like a stable, non-oscillatory system. One of the concerns was that feedback of muscle length (or limb position) would give rise to oscillations at high velocities due to the delays in the reflex loop (Kilmer et al. 1983). Theoretical considerations show that a feedback of velocity is much more favorable for stability. One of the nice properties of the model described by (1) and (2) is that for high velocities the response of the model is mainly determined by velocity. As such, the reflex loop acts like a velocity servo. However, for low velocities the response of the model is determined by muscle length. As a consequence the reflex loop acts like a position servo in these conditions and regulates stiffness of the limb (Houk and Rymer 1981). With these different properties at low and high velocities the model makes the servo stable over the whole range of movements.

References

Abbott BC, Aubert XM (1952) The force exerted by active striated muscle during and after change of length. J Physiol (London) 117:77–86

Aldridge A, Stein RB (1982) Nonlinear properties of stretch reflex studied in the decerebrate cat. J Neurophysiol 47:179–192

Bawa P, Mannard A, Stein RB (1976) Predictions and experimental tests of a visco-elastic muscle model using elastic and inertial loads. Biol Cybern 22:139–145

Bigland B, Lippold OCJ (1954) The relation between force, velocity and integrated electrical activity in human muscles. J Physiol (London) 123:214–224

Brown MC, Goodwin GM, Matthews PBC (1969) After-effects of fusimotor stimulation on the response of muscle spindle primary afferent endings. J Physiol (London) 205:667–694

Carp JS, Boskov D, Rymer WZ (1986) Nonlinear muscle spindle behavior in stretch reflex of the decerebrate cat. Soc Neurosci 12(I):681 (abstr)

Crowe A, Matthews PBC (1964) The effects of stimulation of static and dynamic fusimotor fibres on the response to stretching of the primary endings of muscle spindles. J Physiol (London) 174:109–131

Cussons PD, Hulliger M, Matthews PBS (1977) Effects of fusimotor stimulation on the responses of the secondary

endings of the muscle spindle to sinusoidal stretching. J Physiol (London) 270:835–850
DeLuca CJ, LeFever RS, McCue MP, Xenakis AP (1982a) Behavior of human motor units in different muscles during linearly varying contractions. J Physiol (London) 329:113–128
DeLuca CJ, LeFever RS, McCue MP, Xenakis AP (1982b) Control scheme governing concurrently active human motor units during voluntary contractuons. J Physiol (London) 329:129–142
Edman KAP, Elzinga G, Noble MIM (1976) Force enhancement induced by stretch of contracting single skeletal muscle fibres of the frog. J Physiol (London) 258:95P–96P
Gielen CCAM, Houk JC (1984) Nonlinear viscosity of human wrist. J Neurophysiol 52:553–569
Gielen CCAM, Houk JC, Marcus SL, Miller LE (1984) Viscoelastic properties of the wrist motor servo in man. Ann Biomed Eng 12:599–620
Hasan Z (1983) A model of spindle afferent response to muscle stretch. J Neurophysiol 49:989–1006
Hasan Z, Houk JC (1975a) Analysis of response properties of de-efferented mammalian spindle receptors based on frequency response. J Neurophysiol 38:663–672
Hasan Z, Houk JC (1975b) Transition in sensitivity of spindle receptors that occurs when muscle is stretched more than a fraction of a millimeter. J Neurophysiol 38:673–689
Hill AV (1938) The heat of shortening and theories of contraction. Proc R Soc Ser B 126:136–195
Houk JC (1981) Afferent mechanisms mediating autogenic reflexes. In: Marsan CA, Pompeiano O (eds) Brain mechanisms of perceptual awareness and purposeful behavior. Raven Press, New York, pp 167–181
Houk J, Gielen C (1986) Stiffness versus length control. Proc Int Union Physiol Sci 16:253
Houk JC, Rymer WZ (1981) Neural control of muscle length and tension. In: Brooks VB (ed) Motor control. Handbook of physiology, sect 1, vol I. American Physiological Society, Bethesda, Md, pp 257–323
Houk JC, Singer JJ, Goldman MR (1970) An evaluation of length and force feedback to soleus muscles of decerebrate cat. J Neurophysiol 33:784–811
Houk JC, Harris DA, Hasan Z (1973) Non-linear behavior of spindle receptors. In: Stein RB, Pearson KB, Smith RS, Redford JB (eds) Control of posture and locomotion. Plenum, New York, pp 147–163
Houk JC, Rymer WZ, Crago PE (1981a) Dependence of dynamic response of spindle receptors on muscle length and velocity. J Neurophysiol 46:143–166
Houk JC, Crago PE, Rymer WZ (1981b) Function of the spindle dynamic response in stiffness regulation. A predictive mechanism provided by non-linear feedback. In: Taylor H, Prochazka A (eds) Muscle receptors and movement. MacMillan, London, pp 299–309
Huxley AF (1957) Muscle structure and theories of contraction. Prog Biophys Biophys Chem 7:257–318
Jack JJB, Roberts RC (1978) The role of muscle spindle afferents in stretch and vibration reflexes of the soleus muscle of the decerebrate cat. Brain Res 146:366–372
Jørgensen K (1976) Force-velocity relationship in human elbow flexors and extensors. In: Komi (ed) International series on biomechanics, vol 1A. University Press, pp 145–151
Joyce GC, Rack PMH (1969) Isotonic lengthening and shortening movements of cat soleus muscle. J Physiol (London) 204:475–491
Joyce GC, Rack PMH, Westbury DR (1969) The mechanical properties of cat soleus muscle during controlled lengthening and shortening movements. J Physiol (London) 204:461–474
Julian FJ, Morgan DL (1979) The effect on tension of non-uniform distribution of length changes applied to frog muscle fibres. J Physiol (Lond) 293:379–392
Kilmer W, Kroll W, Pelosi R (1983) On the stability of delay equation models of simple human stretch reflexes. J Math Biol 17:331–349
Lennerstrand G (1968) Position and velocity sensitivity of muscle spindles in the cat. I. Primary and secondary endings deprived of fusimotor activation. Acta Physiol Scand 73:281–299
Lennerstrand G, Thoden U (1968) Dynamic analysis of muscle spindle endings in the cat using length changes of different length-time relations. Acta Physiol Scand 73:234–250
Matthews PBC (1969) Evidence that the secondary as well as the primary endings of the muscle spindles may be responsible for the tonic stretch reflex of the decerebrate cat. J Physiol (Lond) 204:365–393
Matthews PBC (1972) Mammalian muscle receptors and their central actions. Arnold, London
Matthews PBC, Stein RB (1969) The sensitivity of muscle spindle afferents to sinusoidal stretching. J Physiol (Lond) 200:723–743
Oguztoreli MN, Stein RB (1976) The effects of multiple reflex pathways on the oscillations in neuro-muscular systems. J Math Biol 3:87–101
Poppele RE, Bowman RJ (1970) Quantitative description of linear behavior of mammalian muscle spindles. J Neurophysiol 33:59–72
Prochazka A (1981) Muscle spindle function during normal movement. In: Porter R (ed) Neurophysiology IV, vol 25. University Park, Baltimore, Md pp 47–90
Rack PMH (1981) Limitations of somatosensory feedback in control of posture and movement. In: Brooks VB (ed) Motor control. Handbook of physiology, sect 1, vol II. American Physiological Society, Bethesda, Md, pp 229–259
Rack PMH, Ross HF (1984) The tendon of flexor pollicis longus: its effects on the muscular control of force and position at the human thumb. J Physiol (Lond) 351:99–110
Rymer WZ, Hasan Z (1980) Absence of force feedback in soleus muscle of the decerebrate cat. Brain Res 184:203–209
Stein RB (1974) The peripheral control of movement. Physiol Rev 54:215–243
Wei HY, Kripke BR, Burgess PR (1986) Classification of muscle spindle receptors. Brain Res 370:119–126
Zahalak GI (1981) A distribution-moment approximation for kinetic theories of muscular contraction. Math Biosci 55:89–114

Received: October 10, 1986
Accepted in revised form: March 30, 1987

Dr. J. C. Houk
Department of Physiology
Northwestern University
Medical School
303 East Chicago Avenue
Chicago, IL 60611
USA